Visible Light Diagnostics at SPEAR3

Jeff Corbett[a], Weixing Cheng[b], Alan S. Fisher[a], Walter Mok[a] & Stuart Westerman[a]

[a]*SLAC National Accelerator Laboratory, Menlo Park, CA 94306, USA*
[b]*Brookhaven National Laboratory, Upton, NY 11973, USA*

Abstract. The visible light diagnostic beam line at SPEAR3 utilizes dipole radiation extracted through an ID exit port to evaluate electron beam properties at a variety of diagnostic end-stations. The unfocused SR light is collected 17m from the source point by a 150mm diameter, f=2m lens and optically relayed to the appropriate station. For transverse imaging, an image-intensified PiMax camera with 2ns gate allows measurement of fast beam dynamics for either the stored beam or the injected beam. For these applications the visible light is switched into either a standard symmetric-lens transport line or a beam-shaping transport line equipped with cylindrical lenses and a rotating mirror to sweep the beam image across the camera photocathode. A separate two slit stellar-interferometer branch line can resolve the diffraction-limited vertical beam height down to about 10μm. For longitudinal charge profile measurements, the light is switched to a Hamamatsu C5680 streak camera with net system resolution of ~2.5ps rms. In this paper we outline the main photon beam transport line, review the SR beam properties and describe measurement capabilities at each diagnostic station.

TRANSPORT LINE AND PHOTON BEAM PROPERTIES

The SPEAR3 light source features a 10nm-rad emittance electron beam with up to 500mA circulating current. The visible light diagnostic beam line takes dipole radiation ~10mrad into a standard, 1.27T dipole magnet where the source point dimensions are 150 x 20μm and the critical photon energy is 7.6keV. At 500mA the total radiated power into the 3.5x6mrad beam line acceptance is 245W. To reduce beam power on the first Rh-coated Si mirror (M0), the x-ray component is intercepted by a ±0.47mrad GlidCop 'cold finger' extending horizontally across the core of the beam. Hence, as illustrated in Figure 1, both the upper and lower portions of the beam are accessible for observation. This configuration yields the maximum photon flux and the opportunity for transverse beam coherence measurements. The remaining 5W beam power past the cold finger strikes an Rh-coated silicon mirror at 9° incidence yielding ~200μW of UV/visible/IR radiation for diagnostic applications. Both the cold-finger and the M0 mirror reside in SPEAR3 vacuum. The beam then passes through a 1"-thick fused quartz window, propagates through a 3m evacuated beam pipe with an interlocked Pb shutter and enters a He-atmosphere, lead-lined two-bounce mirror box which rejects any stray x-ray component and steers the beam down the center of the optical bench. Similar 1" thick fused silica windows are located at the entrance and exit of the mirror box. At the upstream end of the optical bench the unfocused beam measures 60 x 100mm with a 16mm high cold finger 'dark' stripe across the center. The fwhm opening angle of the visible radiation is about 75% of the vertical beam line acceptance.

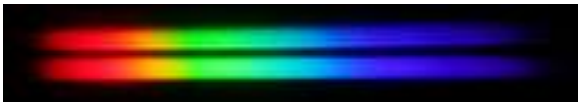

FIGURE 1. Visible beam spectrum with cold finger stripe.

The electromagnetic composition of the visible SR beam is interesting. Above and below the mid-plane the radiation is left/right circularly polarized with power in the σ– and π–polarization components varying as a function of vertical observation angle [1]. Although the mirrors and windows pass λ=250nm-to-near IR radiation, a low-pass UV filter removes radiation below λ=420nm to satisfy the safety requirements. Due to the small source size, the visible component is sufficiently coherent in the transverse direction to enable interferometric measurements of beam size. At a slit separation of ±40mm the visibility of the interference pattern is still about V~0.5 (see below). In the longitudinal direction, a 1nm fwhm bandpass filter yields a coherence length $\lambda^2/\Delta\lambda$ = 400μm or 3 percent of the 14mm (45ps) fwhm pulse length during normal user beam operation.

Similar to conditions in many soft- and hard x-ray beam lines, the photon flux in the visible beam is less than optimum for time-resolved measurements. In a 40nm fwhm portion of the spectrum centered at 550nm (2.2eV), the beam power incident on the optical bench is typically 80nW/ma. Under nominal conditions with 1ma in a single bunch, this translates into a net flux of $2x10^{11}$photons/s or $1.7x10^{5}$photons-per-pass. For short-pulse experiments where the beam intensity must be kept low to minimize bunch-lengthening impedance effects, the single-bunch current is often reduced to values as low as 10μA. Under these conditions the cameras receive only a few thousand photons/pass so analog integration or off-line statistical averaging of many images is required. At the shortest bunch lengths, the filtering must be further reduced to 10nm fwhm to minimize chromatic dispersion effects. Similarly, each injected pulse from the booster synchrotron typically contains 20-50pC electronic charge (10^{8} e^{-}) or an equivalent current of a few 10's of μA, so again the photon flux is low at the diagnostic end-stations. For these measurements, the filters are often removed to increase the photon flux and multiple exposures are acquired on a shot-by-shot basis to resolve the image.

EXPERIMENTAL END-STATIONS

To date, the main applications of the diagnostic beam line have been to measure the longitudinal beam profile as a function of single-bunch current and to image time evolution of the transverse beam distribution during injection and periods of the 'bursting' instability in the short-pulse mode. The injection studies are important for top-up efficiency, protection of ID's and optical tuning of the booster-to-spear transfer line. A third application is to measure vertical beam size with a two-slit interferometer. An additional branch line contains a power meter and/or photo-diode for beam intensity measurements. Due to the need to provide maximum flux to the streak- and gated cameras, the beam is manually 'switched' with mirrors from one branch line to the next.

Streak Camera (Hamamatsu Photonics, C5680 with dual-scan)

Streak cameras are used for a wide range of longitudinal pulse-profile measurements in the accelerator community. The optical path in the SPEAR3 beam line consists of the main f=2m, 150mm diameter lens followed by an f=30mm collimating lens located 30mm behind the resulting virtual source point. A pair of folding mirrors route the parallel beam back up the optical bench to the streak camera. Beam conditioning components include an OD1-5 filter wheel and bandpass filters to reduce chromatic dispersion in the optics. A Leice Acro 10/0.25 objective lens produces a final focus at the entrance the slit of the streak camera. Once inside the camera, visible light is converted to electrons on the photocathode and the pulse is 'streaked' by electrostatic deflection plates to yield a head-to-tail image on a phosphor screen. The CCD camera captures an image as though looking down on the bunch profile in the x-t laboratory frame, or by physically rotating the input beam, imaged side on (y-t plane). In synchroscan mode the streak camera has ~2.5ps rms resolution when 1ps rms synchrotron oscillations are taken into account [2].

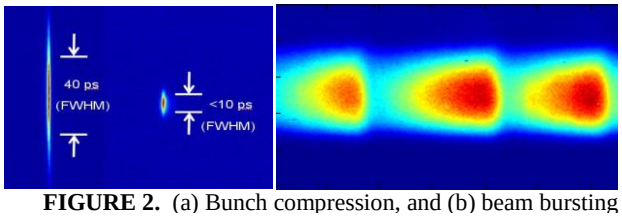

FIGURE 2. (a) Bunch compression, and (b) beam bursting

The primary applications of the streak camera have been to measure bunch length as a function of beam current in different accelerator operational modes [3]. Changes in the longitudinal charge profile as a function of current yield important vacuum chamber and coherent SR impedance data. In the quasi-isochronous 'low-alpha' mode, electron bunches can be compressed by a factor of 4 or more (Figure 2a) but the operation is restricted to low beam current, low photon flux, and consequently long integration times. Jitter in the pulse arrival time and coherent synchrotron oscillations becomes difficult to de-convolve from the raw data.

By operating in 'dual-scan' (slow horizontal axis sweep) it is possible to resolve 'bursting' activity in the longitudinal plane above well-defined single-bunch current thresholds. The image shown in Figure 2b illustrates how the electron beam distribution is spoiled during 'burst' events resulting in a large fraction of SR photons not captured within the acceptance of the diagnostic beam line. This appears as the 'neck' portions of Figure 2b.

In more recent experiments single-turn images of the injected pulse have been captured in the horizontal-time (x-t) plane. Similar to the gated-camera optics, cylindrical lenses are used to expand the incoming beam image horizontally while compressing vertically to maintain time resolution along the vertical (time) axis. In this case, the streak camera MCP is gated synchronously with the corresponding turn of interest as the injected pulse circulates

around the ring. All filters must be removed and images acquired in the multiple exposure mode to obtain sufficient intensity. In the future the streak camera will be used to quantify longitudinal multi-bunch instability thresholds.

Fast-Gated Camera (Roper Scientific, PiMax Camera)

The fast-gated camera system features an MCP image intensifier and 2ns electronic shutter capable of imaging individual electron bunches. Depending on the application, the visible SR beam is directed to the camera photocathode through one of two beam transport lines (a) a symmetric-lens system with source de-magnification of M=0.6 or (b) a cylindrical-lens optical transport line with rotating mirror to sweep the beam image across the photocathode in time. Two interchangeable pick-off mirrors located ~1.2m behind the main f=2m lens are used to switch between optics.

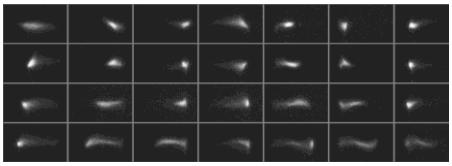

FIGURE 3. Injected beam turn sequence.

The symmetric-lens optics configuration is typically used to image time-dependent beam dynamics in the transverse plane following a deliberate transverse beam excitation or during the first turns of an injected pulse. In each case the beam executes transverse 'betatron' oscillations and the image can cover most of the photocathode area on a turn-by-turn basis. During injection measurements, the single-pass image intensity is weak so all filtering is typically removed. The camera gating sequence is arranged to accumulate multiple exposures per frame for a given turn. By using the 'sequence' acquisition mode, for instance, 50-exposure images can be accumulated for the first 50 turns with the appropriate time-delays relative to the injection trigger. An example of a 'well tuned' injection sequence is shown in Figure 3. Each image in the sequence can be post-processed to evaluate moments of the beam distribution and charge loss.

To monitor stationary beam dynamics, a series of images can be captured in a single camera exposure. Similar to the system developed at PEP-II [4], the beam is first physically rotated by 90° with a vertical periscope and then passed through a pair of cylindrical-lenses with different focal lengths in the horizontal and vertical plane. The resulting image is 'tall' along the vertical axis of the CCD and 'narrow' along the horizontal axis. The net de-magnifications M_x=0.7and M_y=0.02 produce the narrow, vertical stripe in the image plane. As illustrated in Figure 4a, the 'string bean' image is then swept across the camera photocathode using the synchronous rotating-mirror. The beam size modulations that progress from left to right are indicative of quasi-periodic 'bursting' activity observed in short-bunch, high current operation [5]. To capture this effect, the camera was periodically gated to image discrete, non-overlapping snapshots in time, in this case every 130th turn (trigger rate 10kHz). The bursting dynamics is coincident with longitudinal measurements discussed above. Figure 4b shows an example of transient-decay of an injected pulse in the horizontal plane. In this case the shutter was held open and the images overlap during the sweep interval.

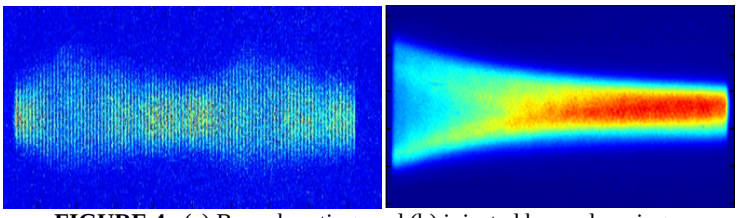

FIGURE 4. (a) Beam bursting, and (b) injected beam damping.

Stellar Interferometer (PointGrey Research, Flea2)

Following the pioneering work of Michelson to measure stellar diameters with Young's two-slit interferometer and the ingenious application to accelerators by Mitsuhashi [6], a similar system was installed at SPEAR3. Like a distant star, the statistically thermal radiation of the small SR beam carries with it a spatial 'degree of coherence' that can be used to infer electron beam size below the normal diffraction limit that applies to standard imaging techniques. As shown in Figure 5, the two-slit mask is inserted in the unfocused beam just upstream of the f=2m lens to generate an interference pattern with fringe visibility $V = (I_{\max} - I_{\min})/(I_{\max} + I_{\min})$. The VanCittert-Zernike theorem states that under sufficiently linear conditions the Fourier transform of the fringe visibility plotted as a

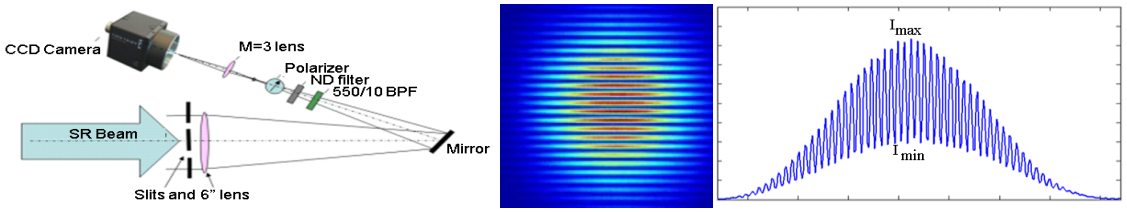

FIGURE 5. (a) Interferometer configuration, (b) interference pattern and (c) lineout for beam size analysis.

function of slit separation yields the spatial intensity profile of the incoherent source. For Gaussian beams, the transform pair is particularly simple and the slits can be set to a single, fixed separation distance to infer beam size. In SPEAR3 however, the high degree of coherence in the visible beam requires a large slit separation to obtain optimum visibility values of V~0.5 which in turn drives up the interference modulation frequency. As seen in Figure 5c, the interference pattern can be difficult to resolve on the 4.65μm pixel CCD camera (PointGrey, Flea2) without introducing further magnification of the image. The CCD camera is controlled through a Matlab graphical interface which displays both the raw image and the interference pattern with numerical fit. In principle, the interferometer resolution can suffer from wavefront distortion on the low incidence-angle M0 mirror and mechanical vibration of the optical bench but in practice the system can resolve vertical beam sizes of order 10μm.

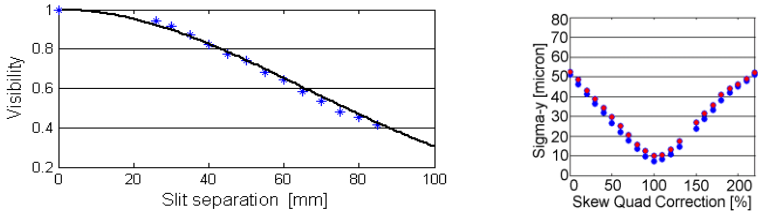

FIGURE 6. (a) Visibility vs. slit separation and (b) beam size vs coupling.

Figure 6 shows an example of visibility plotted as a function of slit separation. A Gaussian curve fit to data yields an rms value of σ_d=64mm or a vertical beam size of σ_y=23.2μm. Figure 6b shows measurements of vertical beam size taken with fixed slit separation and variable x-y coupling on the electron beam [7]. Simultaneous x-ray pinhole measurements are shown in red.

SUMMARY

The visible diagnostic beam line in SPEAR3 has produced valuable information for accelerator impedance, short-pulse operation, injection transients, impulse-driven beam dynamics and vertical beam size. The three main branch lines (streak camera, fast-gated camera and interferometer) are fully functioning and are expected to produce further results to assist in top-off operation, short-pulse research and instability studies.

ACKNOWLEDGMENTS

The authors would like to thank the SSRL accelerator operations and beam line staff and many summer students for extensive support. C.Limborg and A.Ringwall designed the original beam line during the SPEAR3 upgrade project. A.Lumpkin and J.Sebek made important contributions to measurement and analysis of streak camera data.

REFERENCES

1. A. Hofmann, "The Physics of Synchrotron Radiation", Cambridge University Press, 2004.
2. W.Cheng, A.S.Fisher and J.Corbett, 'Streak Camera Measurements in PEP-II and Variable Optics in SPEAR3', BIW08, Lake Tahoe, CA (2008).
3. J. Corbett, *et al*, 'Short-Bunch Measurements in SPEAR3', PAC 2009, May 4-8, Vancouver, Canada.
4. A.S. Fisher, *et al.*, 'Turn-by-Turn Imaging of the Transverse Beam Profile in PEP-II', BIW06, Batavia, IL.
5. W. Cheng, *et al*, 'Fast-Gated Camera Measurements in SPEAR3', PAC 2009, May 4-8, Vancouver, Canada.
6. T. Mitsuhashi, 'Beam Profile and Size Measurement by SR Interferometer' in *Beam Measurements*, Ed. By S. Kurokawa, et al, p. 399-427, World Scientific (1999).
7. J. Corbett, *et al*, 'Interferometer Beam Size Measurements in SPEAR3', PAC 2009, May 4-8, Vancouver, Canada.